Advanced GMSK Demodulation Architectures Based on Laurent Decomposition: Theory and Performance Analysis

Iliass Sijelmassi
Department of Digital Sciences
INP ENSEEIHT
Toulouse, France
2nd Year SN

***Abstract*—Gaussian Minimum Shift Keying (GMSK) is the modulation standard for Global System for Mobile Communications (GSM) and various satellite communication protocols due to its spectral efficiency and constant envelope properties. However, the inherent inter-symbol interference (ISI) introduced by the Gaussian shaping filter necessitates complex equalization at the receiver. This paper presents a comprehensive analysis of GMSK demodulation techniques founded on Laurent Decomposition, which linearizes the Continuous Phase Modulation (CPM) signal into a sum of Pulse Amplitude Modulation (PAM) waveforms. We mathematically derive the decomposition for modulation indices $h = 0.5$ and analyze receiver architectures ranging from optimal Maximum Likelihood Sequence Estimation (MLSE) to reduced-complexity sub-optimal designs. Simulation results comparing Bit Error Rate (BER) against Signal-to-Noise Ratio (SNR) for varying BT products demonstrate that improved sub-optimal algorithms offer a viable trade-off between computational cost and reception reliability.**

***Index Terms*—GMSK, Laurent Decomposition, CPM, Viterbi Algorithm, MLSE, GSM, Satellite Communications.**

I. Introduction

In modern telecommunications, the physical layer is tasked with transforming digital information into analog waveforms suitable for transmission through lossy channels. While analog modulation schemes (AM, FM) suffice for voice or basic audio, digital modulation is required to maximize data throughput while maintaining an acceptable Bit Error Rate (BER).

Among digital modulation schemes, Continuous Phase Modulation (CPM) holds a distinct advantage due to its phase continuity, which results in a compact power spectrum. Gaussian Minimum Shift Keying (GMSK), a specific subclass of CPM, is extensively used in the GSM 2G cellular standard, CDPD (Cellular Digital Packet Data), and CCSDS satellite communication standards [1].

The primary appeal of GMSK lies in its constant envelope property. Unlike Quadrature Amplitude Modulation (QAM) or shaped QPSK, GMSK carries information solely in the phase variations, not the amplitude. This allows the use of non-linear, power-efficient amplifiers (Class C) at the transmitter, significantly extending battery life for mobile terminals [2].

However, the Gaussian filter used to shape the frequency pulse introduces controlled Inter-Symbol Interference (ISI). While this tightens the spectral bandwidth, it complicates the receiver design. The optimal receiver for such signals requires Maximum Likelihood Sequence Detection (MLSE), typically implemented via the Viterbi algorithm.

To mitigate the complexity of non-linear CPM receivers, Pierre A. Laurent proposed a linearization method in 1986 [3]. This method decomposes the GMSK signal into a superposition of amplitude-modulated pulses (PAM). This paper explores this decomposition, proposing and analyzing three demodulation architectures:

1) **Optimal Demodulation:** Utilizing the full Laurent expansion.
2) **Sub-optimal Demodulation:** Truncating the expansion to the dominant pulse.
3) **Improved Sub-optimal Demodulation:** Retaining the two most significant pulses to balance performance and complexity.

II. GMSK Signal Model

GMSK is derived from Minimum Shift Keying (MSK) by passing the modulating data stream through a Gaussian low-pass filter prior to frequency modulation.

A. Standard Expression

The signal $s(t)$ can be represented in its quadrature form as:

$$s(t) = a_I(t)\cos\left(\frac{\pi t}{2T}\right)\cos(2\pi f_c t) - a_Q(t)\sin\left(\frac{\pi t}{2T}\right)\sin(2\pi f_c t) \tag{1}$$

where $a_I(t)$ and $a_Q(t)$ represent the in-phase and quadrature data streams, T is the symbol duration, and f_c is the carrier frequency.

More generally, as a CPM signal, GMSK is defined by:

$$s_c(t,\alpha) = \sqrt{\frac{2E}{T}}\cos(2\pi f_c t + \phi(t,\alpha)) \tag{2}$$

where E is the symbol energy and $\alpha = \{..., \alpha_{-1}, \alpha_0, \alpha_1, ...\}$ is the sequence of independent binary data symbols $\alpha_i \in \{-1, +1\}$.

The information-bearing phase $\phi(t, \alpha)$ is given by:

$$\phi(t, \alpha) = 2\pi h \sum_{k=-\infty}^{\infty} \alpha_k q(t - kT) \tag{3}$$

For GMSK, the modulation index is fixed at $h = 0.5$. The phase response $q(t)$ is the integral of the frequency pulse $g(t)$:

$$q(t) = \int_{-\infty}^{t} g(\tau) d\tau \tag{4}$$

B. The Gaussian Filter

The distinct characteristic of GMSK is the Gaussian frequency pulse $g(t)$, defined as:

$$g(t) = \frac{1}{2T} \left[Q\left(2\pi B \frac{t - T/2}{\sqrt{\ln 2}} \right) - Q\left(2\pi B \frac{t + T/2}{\sqrt{\ln 2}} \right) \right] \tag{5}$$

where $Q(x)$ is the Gaussian Q-function. In the context of the provided source material, this is expressed using the error function $\text{erf}(x)$ as:

$$g_0(t) = \frac{1}{K} \left[\text{erf}(\beta_0(t)) - \text{erf}(\beta_m(t)) \right] \tag{6}$$

where:

$$\beta_0(t) = C_0 \left[\frac{t}{T} + \frac{1}{2} \right] \tag{7}$$

$$\beta_m(t) = C_0 \left[\frac{t}{T} - \frac{1}{2} \right] \tag{8}$$

$$C_0 = BT\pi \sqrt{\frac{2}{\ln 2}} \tag{9}$$

The BT product (Bandwidth-Time product) is a critical design parameter. A lower BT (e.g., $BT = 0.3$ for GSM) results in a narrower spectrum but higher ISI, as the pulse spreads over multiple symbol periods. A higher BT (e.g., $BT = 0.5$) reduces ISI but occupies more bandwidth.

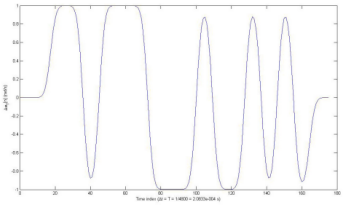

Fig. 1. GMSK Signal Phase Trajectories for $BT = 0.3$. The smoothing effect of the Gaussian filter is evident compared to sharp MSK transitions.

III. Laurent Decomposition

The non-linear relationship between the data sequence α and the signal $s(t)$ in Equation (2) complicates linear detection. Pierre Laurent's breakthrough was demonstrating that any binary CPM signal with non-integer modulation index can be expressed as a sum of 2^{L-1} PAM signals [4].

A. General Decomposition

The Laurent representation is given by:

$$s(t) = \sum_{k=-\infty}^{\infty} \sum_{m=0}^{M-1} a_{k,m} h_m(t - kT) \tag{10}$$

Here, $M = 2^{L-1}$ is the number of PAM components, where L is the correlation length of the frequency pulse (the duration over which $g(t)$ is non-zero).

The components are:

- $h_m(t)$: The real-valued Laurent pulses.
- $a_{k,m}$: The complex-valued pseudo-symbols.

The pulses $h_m(t)$ are constructed from the basic phase response:

$$h_m(t) = \prod_{l=0}^{L-1} c\left(t + lT + \gamma_{m,l} LT\right) \tag{11}$$

where the indices $\gamma_{m,l}$ are derived from the binary representation of the index m.

B. Specific Case: $L = 2$

For many practical GMSK implementations (including $BT = 0.5$), the pulse duration can be approximated by $L = 2$. This simplifies the summation to just two components ($M = 2^{2-1} = 2$):

$$s(t) \approx \sum_{k} a_{k,0} h_0(t - kT) + \sum_{k} a_{k,1} h_1(t - kT) \tag{12}$$

The main pulse $h_0(t)$ (often denoted C_0) contains the vast majority of the signal energy, while $h_1(t)$ (C_1) captures the detailed phase variations and ISI.

The pseudo-symbols are defined recursively:

$$a_{k,0} = j^{k+1} \prod_{n=0}^{k} \alpha_n \tag{13}$$

$$a_{k,1} = j^{k+1} \alpha_k \prod_{n=0}^{k-2} \alpha_n \tag{14}$$

Note that these pseudo-symbols are correlated, which is a property exploited by the Viterbi algorithm.

C. Energy Distribution

The validity of using Laurent decomposition for simplified receivers depends on the energy concentration.

- For $BT = 0.5, L = 2$: h_0 contains $\approx 97.8\%$ of the energy.
- For $BT = 0.3, L = 3$: h_0 contains $\approx 95.7\%$ of the energy, and h_1 contains $\approx 4.2\%$.

The negligible energy in pulses $h_2, h_3, \ldots$ for $L \geq 3$ justifies truncating the series in Equation (10) for sub-optimal receiver designs.

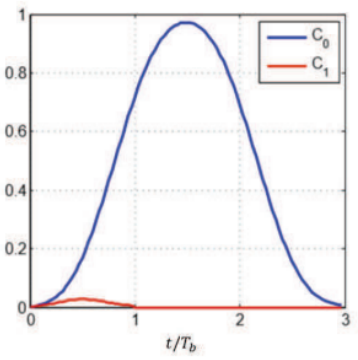

Fig. 2. Laurent Pulses C_0 (blue) and C_1 (red) for $BT = 0.5$. Note that C_0 spans $3T$ while C_1 is significantly smaller.

IV. Receiver Architectures

We examine the transmission over an Additive White Gaussian Noise (AWGN) channel where the received signal is:

$$r(t) = s(t) + n(t) \tag{15}$$

where $n(t)$ is the noise component with spectral density $N_0/2$.

A. Optimal MLSE Receiver

The optimal receiver maximizes the likelihood of the received sequence. Using the Laurent decomposition, this is equivalent to maximizing the log-likelihood function:

$$\Lambda(\tilde{\alpha}) = \text{Re}\left\{\int_{-\infty}^{\infty} r(t)\tilde{s}^*(t)dt\right\} \tag{16}$$

Substituting the Laurent expansion:

$$\Lambda = \text{Re}\left\{\sum_k \sum_m \tilde{a}^*_{k,m} \int r(t)h_m(t-kT)dt\right\} \tag{17}$$

The integral term represents a bank of matched filters. The optimal receiver consists of: 1. A bank of M matched filters, each matched to $h_m(t)$. 2. Sampling at $t = kT$. 3. A Viterbi processor operating on the trellis defined by the memory of the modulation.

For $BT = 0.3$, the effective memory length is significant. If we assume $L = 3$, the number of states in the Viterbi trellis is $S = 2^{L-1} = 4$, or higher depending on the specific implementation of the phase states [5].

B. Sub-optimal Receiver (AMOP)

The "Approximate Mean Output Power" (AMOP) or simplified receiver relies on the observation that $h_0(t)$ dominates. By setting $h_m(t) = 0$ for $m > 0$, we approximate the GMSK signal as a linear PAM signal:

$$s(t) \approx \sum_k a_{k,0}h_0(t-kT) \tag{18}$$

This allows the receiver to use a *single* matched filter adapted to $h_0(t)$. The Viterbi algorithm still resolves the correlation between symbols $a_{k,0}$, but the branch metric calculation is significantly simplified. The complexity reduction is substantial, but performance degrades at low SNR due to the un-modeled energy in $h_1(t)$.

C. Improved Sub-optimal Receiver

To bridge the gap between complexity and performance, particularly for $BT = 0.3$ where the second pulse carries $\approx 4\%$ of the energy, we use an improved model. The receiver utilizes two matched filters (h_0 and h_1). The metric calculation in the Viterbi algorithm incorporates the contributions from both pulses:

$$\lambda_k = \text{Re}\left\{a^*_{k,0}y_{k,0} + a^*_{k,1}y_{k,1}\right\} \tag{19}$$

where $y_{k,m}$ is the output of the filter matched to $h_m(t)$. This recovers the majority of the "interference" energy treated as noise in the simple sub-optimal case.

V. Performance Analysis and Simulation

Simulations were conducted to evaluate the Bit Error Rate (BER) as a function of E_b/N_0 (SNR) for the three architectures.

A. Simulation Setup

- **Modulation:** GMSK with $BT = 0.3$ (GSM standard) and $BT = 0.5$.
- **Channel:** AWGN.
- **Demodulators:** Optimal (All pulses), Sub-optimal (Pulse C_0 only), Improved (Pulses $C_0 + C_1$).
- **Viterbi Traceback:** 15 symbols.

B. Results for BT = 0.3

Figure 3 (derived from source Fig 2.6) illustrates the performance.

- The **Optimal Algorithm** (blue) sets the benchmark, achieving a BER of 10^{-3} at approximately 7 dB SNR.
- The **Sub-optimal Algorithm** (red) shows a degradation of nearly 2-3 dB. This is expected as the $BT = 0.3$ filter creates significant ISI captured by the neglected h_1 pulse.
- The **Improved Algorithm** (yellow) performs between the two, recovering approximately 1.5 dB of the loss incurred by the sub-optimal method.

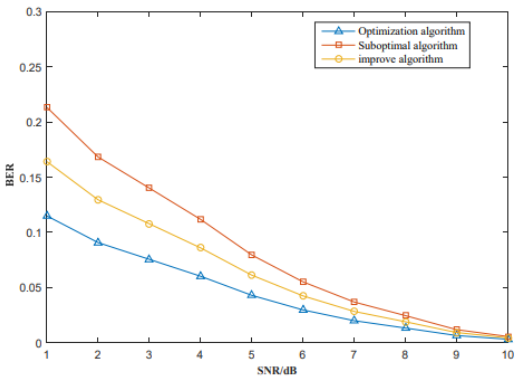

Fig. 3. BER vs. SNR for $BT = 0.3$. The improved algorithm significantly outperforms the basic sub-optimal approach.

C. Results for BT = 0.5

For $BT = 0.5$ (source Fig 2.7), the spectral lobes are wider, and ISI is lower.

- The energy in h_1 drops to $\sim 2\%$.
- Consequently, the performance gap between the Optimal and Sub-optimal receivers narrows.
- The Sub-optimal receiver becomes a very attractive choice for $BT = 0.5$ applications (like CDPD) as the hardware savings outweigh the marginal SNR penalty.

VI. Comparison with QPSK

To contextualize GMSK, we compare it with Quadrature Phase Shift Keying (QPSK).

A. Spectral Efficiency

GMSK provides excellent spectral roll-off compared to QPSK. As shown in the spectral density comparison (Fig. 3.1 in source), GMSK's side lobes decay much faster than NRZ-QPSK. This reduces Adjacent Channel Interference (ACI), allowing tighter channel spacing in cellular networks.

B. Amplifier Linearity (PAPR)

- **QPSK:** When filtered to limit bandwidth, QPSK exhibits a non-constant envelope (high Peak-to-Average Power Ratio - PAPR). This requires linear amplifiers (Class A or AB) to prevent spectral regrowth, which are energetically inefficient (typically 20-30% efficiency).
- **GMSK:** Being constant envelope, GMSK allows the use of Class C amplifiers, which can achieve efficiencies approaching 70-80%. This is the deciding factor for its adoption in mobile handsets [6].

C. Complexity

QPSK can be demodulated with a simple linear receiver. GMSK requires sequence estimation (Viterbi) to remove ISI, making the digital baseband processing significantly more complex. However, with Moore's Law, the cost of digital complexity has fallen drastically compared to the cost of analog power inefficiency, validating the GMSK design choice.

VII. Conclusion

This paper analyzed the application of Laurent Decomposition to GMSK signals. We demonstrated that decomposing the complex CPM signal into linear PAM components allows for flexible receiver designs. The decomposition reveals that GMSK with $BT = 0.3$ is heavily dominated by the first two Laurent pulses.

Our analysis confirms that while a single-pulse sub-optimal receiver is computationally efficient, it suffers noticeable performance degradation in narrow-band scenarios ($BT = 0.3$). The proposed "Improved Sub-optimal" receiver, which incorporates the second Laurent pulse, offers an excellent engineering compromise, recovering a significant portion of the signal energy with only a modest increase in trellis complexity. This balance makes it highly suitable for modern software-defined radio (SDR) implementations of legacy GSM and satellite protocols.

Acknowledgment

The author thanks the faculty of INP ENSEEIHT for their guidance in the "Couches Physiques" curriculum.

References

[1] CCSDS, "Radio Frequency and Modulation Systems–Part 1: Earth Stations and Spacecraft," Recommended Standard, CCSDS 401.0-B-30, 2020.

[2] J. D. Laster, "Robust GMSK Demodulation Using Demodulator Diversity and BER Estimation," Virginia Tech, 1997.

[3] P. A. Laurent, "Exact and Approximate Construction of Digital Phase Modulations by Superposition of Amplitude Modulated Pulses (AMP)," *IEEE Transactions on Communications*, vol. 34, no. 2, pp. 150-160, 1986.

[4] F. Teng, Y. Liao, and Y. Li, "GMSK Coherent Demodulation Technology based on Laurent Decomposition," *International Conference on Communications*, 2018.

[5] O. Kislal, "GMSK Modulator/Demodulator Design and Implementation on FPGA for Cube Satellites," Bogazici University, Master Thesis.

[6] A. Egjam, "GMSK Modulation," University of South Wales, Technical Report.

[7] C. Piat-Durozoi, "Nouvelle forme d'onde et récepteur avancé pour la télémesure des futurs lanceurs," INP Toulouse, PhD Thesis.